



Carex sect. *Rhynchoyctis* (Cyperaceae): a Miocene subtropical relict in the Western Palaearctic showing a dispersal-derived Rand Flora pattern

Mónica Míguez¹ , Berit Gehrke², Enrique Maguilla¹ , Pedro Jiménez-Mejías^{3,†}  and Santiago Martín-Bravo^{1,†}

¹Botany Area, Department of Molecular Biology and Biochemical Engineering, Universidad Pablo de Olavide, ES-41013 Seville, Spain, ²Johannes Gutenberg-Universität, Mainz, Germany, ³New York Botanical Garden, Bronx, NY, USA

ABSTRACT

Aim To evaluate how Cenozoic climate changes shaped the evolution and distribution of *Carex* section *Rhynchoyctis*.

Location Western Palaearctic and Afrotropical regions (Rand Flora pattern).

Methods DNA regions ITS, ETS (nuclear), *matK* and *rpl32-trnL*^{UAG} (plastid) were amplified for 86 samples of species from section *Rhynchoyctis*. Phylogenetic and phylogeographical relationships were inferred using maximum parsimony, Bayesian inference and coalescent-based species tree approaches. Divergence times and ancestral areas were also inferred.

Results *Carex* section *Rhynchoyctis* is a clade that diversified during the middle Miocene in Europe. Most cladogenesis events date to the middle and late Miocene. The Afrotropical group seems to have originated from a colonization event from Europe that occurred in the late Miocene.

Main conclusions Species of the section *Rhynchoyctis* in the Western Palaearctic are Miocene relicts. Late Miocene-Pliocene aridification of the Mediterranean rather than the more commonly reported Pleistocene glaciations seems to have shaped the phylogeography of the group. Putative Miocene-Pliocene refugia were probably located in the Mediterranean peninsulas and islands, as well as in the eastern shores of the ancient Paratethys Sea. The colonization of Africa could have been facilitated by Miocene-Pliocene global cooling.

Keywords

ancestral area reconstruction, biogeography, disjunction, estimation of divergence times, Paratethys, Cenozoic relict

*Correspondence: Mónica Míguez. Botany area, Department of Molecular Biology and Biochemical Engineering, Universidad Pablo de Olavide, ctra. de Utrera km 1, 41013, Seville, Spain.

E-mail: mmigrio@upo.es

†Both authors contributed equally to the senior authorship.

INTRODUCTION

In contrast to the number of studies addressing the effects of Pleistocene glaciations on the phylogeography of plants, there are very few studies addressing in detail the effect of Cenozoic climate changes on plant distributions in the Western Palaearctic (e.g. Valtueña *et al.*, 2012; Chen *et al.*, 2014). Climate changes during the Cenozoic were characterized by a transition from the humid and warmer Eocene conditions to the much cooler and xeric climate of the Miocene and Pliocene (Milne & Abbott, 2002). Geodynamic movements occurring in the Western Mediterranean region were responsible for the isolation of the Mediterranean basin from the Atlantic Ocean, causing what has been called the Messinian

salinity crisis (5.96–5.33 Ma; Krijgsman *et al.*, 1999). The impact of Mediterranean drying had important effects, not only on the Western Palaearctic but also across the entire Northern Hemisphere (Weijermars, 1988). The effects were also substantial in Africa where the summer monsoon was drastically reduced by the shrinkage of Tethys Sea, causing the Sahara Desert to progressively form during the Tortonian Age (11.6–7.2 Ma) (Zhang *et al.*, 2014) until its definitive establishment 2 or 3 Ma (Kroepelin, 2006). These processes altered the composition and distribution of Northern Hemisphere flora. The majority of Cenozoic tropical elements disappeared from most of the Western Palaearctic before the Pleistocene glaciations, remaining in a few southern refugial locations such as the Eastern Mediterranean and Black Sea

basins (Milne & Abbott, 2002; Médail & Diadema, 2009). It has been argued that only a few taxa persisted in the westernmost part of the Palaearctic, e.g. in the Macaronesian archipelagos (Kondrakov *et al.*, 2015). Nevertheless, there is growing evidence of a Cenozoic origin for species in the Western Mediterranean (e.g. Casimiro-Soriguer *et al.*, 2010; Fernández-Mazuecos *et al.*, 2014, 2016; García-Castaño *et al.*, 2014).

Late Cenozoic climate changes may also have played a role shaping the Rand Flora pattern (Pokorný *et al.*, 2015). The Rand Flora pattern is characterized by the current distributions of related taxa tracing disjunct localities around the margin of continental Africa and adjacent archipelagos (Christ, 1910). Two hypotheses are usually invoked to explain the origin of the Rand Flora: (1) Vicariance: the observed pattern is the remains of a continental flora widely distributed in the past. The original distribution was fragmented due to the increased aridity since the Miocene and restricted to peripheral areas that acted as refugia (Sanmartín *et al.*, 2010; Mairal & Sánchez-Meseguer, 2012). (2) Long-distance dispersal between different parts of Africa (Mairal & Sánchez-Meseguer, 2012; Alarcón *et al.*, 2013).

Carex section *Rhynchocystis* Dumort. (*Rhynchocystis* herein) is a small clade comprising only five species (Table 1). Previous molecular analyses (Global *Carex* Group, 2016) have shown the phylogenetic placement of this section within subgenus *Carex* in a well-supported clade together with sections *Sylvaticae* Rouy, *Ceratocystis* Dumort., *Spirostachyae* (Drejer) Bailey and *Rostrales* Meinsh. *Rhynchocystis* shows a biogeographically interesting range, characterized by a Northern–Southern Hemisphere disjunction coupled with a Rand Flora-like pattern (Fig. 1), with species distributed either in the Western Palaearctic (temperate Europe, Mediterranean basin and Macaronesia; i.e. *C. microcarpa*, *C. pendula*) or in sub-Saharan Africa (*C. bequaertii*, *C. mossii*, *C. penduliformis*). This biogeographical pattern is also displayed by other closely related sections in the genus: *Spirostachyae* (Escudero *et al.*, 2009; Martín-Bravo & Escudero, 2012), *Ceratocystis* (Jiménez-Mejías *et al.*, 2012a) and *Sylvaticae* (Martín-Bravo *et al.*, 2013). The age of the clade can be traced back to the early Miocene, given reports of morphologically similar fossil species from central Europe (*C. limosoides* Negru and *C. plicata* Lañc.-Šrod.; reviewed in Jiménez-Mejías *et al.*, 2016).

In this article, we aim to (1) reconstruct the phylogenetic relationships within *Rhynchocystis*; (2) evaluate the possible ancestral areas for the section and its main clades and species; and (3) evaluate the relative contribution of Cenozoic climate changes in shaping the evolution and distribution of the section, with emphasis on the Rand Flora disjunction pattern.

MATERIALS AND METHODS

Sampling

A total of 86 samples (see Table S1 in Appendix S1 in Supporting Information) from *Rhynchocystis* were included in

the molecular study: 10 of *C. bequaertii*, five of *C. microcarpa*, 10 of *C. mossii*, 58 of *C. pendula* and three of *C. penduliformis* (Table S1 in Appendix S1). We included two species from each of the closely related sections *Sylvaticae* (*C. sylvatica* Huds., *C. rainbowii* Luceño, Jim.Mejías, M. Escudero & Martín-Bravo), *Spirostachyae* (*C. distans* L., *C. punctata* Gaud.) and *Ceratocystis* (*C. demissa* Hornem., *C. flava* L.), as well as from the more distant section *Phacocystis* (*C. reuteriana* Boiss., *C. trinervis* Dumort.) as outgroup.

A distribution map for *Rhynchocystis* species was created using ArcGIS 10.2 (ESRI, Redlands, California, USA) based on confirmed herbarium vouchers (Míguez *et al.*, unpublished data) and floras (see references in Fig. 1).

DNA extractions, amplification and sequencing

DNA was extracted from silica-dried material collected in the field or herbarium specimens (B, E, M, MA, MHA, MADJ, UPOS, UPS, US, P, PRE, SEV, SS, TUM, Z; abbreviations following Thiers, 2015), using the DNeasy Plant Mini Kit (Qiagen, California, USA). We amplified and sequenced the nuclear ribosomal (nrDNA) internal transcribed spacer (ITS) and external transcribed spacer (ETS) regions. The variability of five plastid regions (ptDNA) was tested (*rpl32-trnL*^{UAG}, *matK*, *yef6-psbM*, *rps16*, *5'trnK intron*) in a pilot study on a subset of samples (results not shown). The most variable plastid regions were *matK* and *rpl32-trnL*^{UAG}, which were subsequently sequenced for the complete sampling. These regions have been successfully used to address phylogenetic relationships within *Carex*, including groups closely related to *Rhynchocystis* (Starr *et al.*, 2009; Jiménez-Mejías *et al.*, 2011). PCR conditions and primers followed those described in Global *Carex* Group (2016) for ITS, ETS and *matK*, and Shaw *et al.* (2007) for *rpl32-trnL*^{UAG}.

Products were cleaned using enzymatic purification ExoSAP-IT (USB Corporation, Ohio, USA) following the manufacturer's protocols and sequenced using Big Dye Terminator v. 2.0 (Applied Biosystems, Little Chalfont, UK) run on an Applied Biosystems Prism Model 3700 automated sequencer. Raw sequences were edited, assembled, aligned and manually corrected using GENEIOUS 6.1.7 (Biomatters, Auckland, New Zealand). IUPAC symbols were used to represent nucleotide ambiguities in ITS and ETS sequences.

Phylogenetic analyses

Five matrices were used for phylogenetic analyses: (1) ITS, (2) ETS, (3) combined nrDNA (ITS and ETS), (4) combined ptDNA (*matK* and *rpl32-trnL*^{UAG}), and (5) combined nrDNA-ptDNA. We performed maximum parsimony (MP) and Bayesian inference (BI) analyses following Maguilla *et al.* (2015). Gene trees were compared prior to concatenation and checked for incongruences of supported nodes with Bayesian posterior probabilities >0.95 and parsimony bootstrap support >75% (Gehrke *et al.*, 2010). For the combined nrDNA and combined ptDNA matrices, we excluded those

Table 1 Summarized taxonomic treatments of *Carex* sect. *Rhynchocystis* at species level. Left column includes the list provided by Global *Carex* Group (2016), which has been followed in this work.

Global <i>Carex</i> Group (2016)	Kükenthal (1909)	Egorova (1999)	Natural distribution
Section <i>Rhynchocystis</i> Dumort.	Section <i>Maximae</i> Asch.	Section <i>Rhynchocystis</i> Dumort.	
<i>C. bequaertii</i> De Wild.	<i>C. petitiiana</i> A. Rich. ¹	<i>C. bequaertii</i> De Wild <i>C. petitiiana</i> A. Rich1	E Tropical Africa
<i>C. microcarpa</i> Bertol. ex Moris	<i>C. microcarpa</i> Bertol. ex Moris	<i>C. microcarpa</i> Bertol. ex Moris	Corsica, Sardinia and C Italy
<i>C. mossii</i> Nelmes		<i>C. mossii</i> Nelmes	E South Africa
<i>C. pendula</i> Huds.	<i>C. pendula</i> Huds.	<i>C. pendula</i> Huds.	Europe, North to 58°N; southwestern Asia; northwestern Africa; Azores and Madeira
<i>C. penduliformis</i> Cherm.	<i>C. joorii</i> L.H. Bailey ² <i>C. shortiana</i> Dewey ² <i>C. jaluensis</i> Kom. ³ <i>C. maculata</i> Boott ³ <i>C. vicinalis</i> Boott ³		Madagascar

¹The *C. petitiiana* A. Rich type collection contained mixed material of *C. petitiiana* as currently delimited (section *Spirostachyae*), and *C. bequaertii* (Nelmes, 1940); following Gehrke's (2010) lectotypification, the name for the species from section *Rhynchocystis* formally became *C. bequaertii*.

²The North American *C. joorii* and *C. shortiana* were transferred to sections *Glaucescentes* and *Shortianae*, respectively (Reznicek, 2001); which is supported by recent phylogenies (Global *Carex* Group, 2016).

³The Asian *C. jaluensis* and *C. maculata* have been transferred to section *Anomalae* (Dai & Koyama, 2010); accordingly, the character displayed by *C. vicinalis*, endemic to S India (e.g. bracts sheathless), places this species as allied to section *Anomalae* too, instead of to section *Rhynchocystis*, as already recognized in the lists from Global *Carex* Group (2016).

samples that lacked one of the DNA regions, whereas for the combined nrDNA-ptDNA matrix, only terminals which lacked more than one DNA region were discarded, resulting in 8% missing data (7.72% missing in ETS, 8.8% in ITS, 8.2% in *matK* and 7.64% in *rpl32-trnL*^{UAG}).

Four matrices were used for a coalescent-based species tree analysis performed using STAR (Liu *et al.*, 2009) as implemented in the STRAW web server (Shaw *et al.*, 2013). Post-burn-in gene trees from the MRBAYES analyses of the ETS, ITS, *matK* and *rpl32-trnL*^{UAG} regions were used independently, excluding samples lacking any of the four DNA regions. We failed to amplify some markers for *C. penduliformis* due to poor DNA quality yielded by the sampled herbarium specimens. Due to the lack of ITS sequences for *C. Penduliformis*, we performed another species tree analysis excluding the ITS region to retain this taxon in the analysis.

Haplotype and ribotype network

We obtained genealogical relationships among ptDNA haplotypes and nrDNA ribotypes using ptDNA and nrDNA combined matrices, respectively. Statistical parsimony was performed using TCS 1.21 (Clement *et al.*, 2000). The ptDNA matrix was split to analyse *C. pendula* haplotypes independently, following the phylogenetic results, which showed a large genetic divergence between *C. pendula* and the other species (see Results). Ribotypes were analysed keeping all samples in the same matrix. Maximum numbers of differences resulting from single substitutions among haplotypes and ribotypes was calculated with 95% confidence

limits. Informative indels were coded as a presence/absence character in the matrices.

Divergence-time estimation

We constructed a matrix of 64 sequences: six from *Rhynchocystis* (Appendix S3); 55 from the rest of *Carex*, constituting a representative sampling of the main *Carex* lineages; and three from outgroups, based on Global *Carex* Group (2016). The matrix consisted of 64 combined ETS, ITS and *matK* sequences with an aligned length of 1696 sites. A dated phylogeny was estimated using BEAST 1.8.0 (Drummond *et al.*, 2012), using an uncorrelated log-normal relaxed clock. Two fossils were used as calibration points, following Jiménez-Mejías *et al.* (2016): *Carex colwellensis* Chandler, 38–33.9 Ma (Priabonian, late Eocene), the oldest reliable known fossil ascribable to *Carex*; and *Carex limosoides*, 23.03–15.97 Ma (early Miocene), the oldest fossil considered to belong to *Rhynchocystis*. Since *C. colwellensis* fossil achene and associated utricle remains (Chandler, 1963; Jiménez-Mejías *et al.*, 2016) display synapomorphies considered unique of modern *Carex*, we placed it at *Carex* crown group (Parham *et al.*, 2012). The fossil *C. limosoides* is considered to belong to *Rhynchocystis*, as it displays the typical combination of carpological characters of this section (Jiménez-Mejías *et al.*, 2016). However, we cannot rule out that these characters have appeared before the crown radiation. Accordingly, to be cautious and avoid an age overestimation for our study group, we placed it at *Rhynchocystis* stem node. Fossil priors were implemented as a log-normal distribution since this distribution is considered the most appropriate for

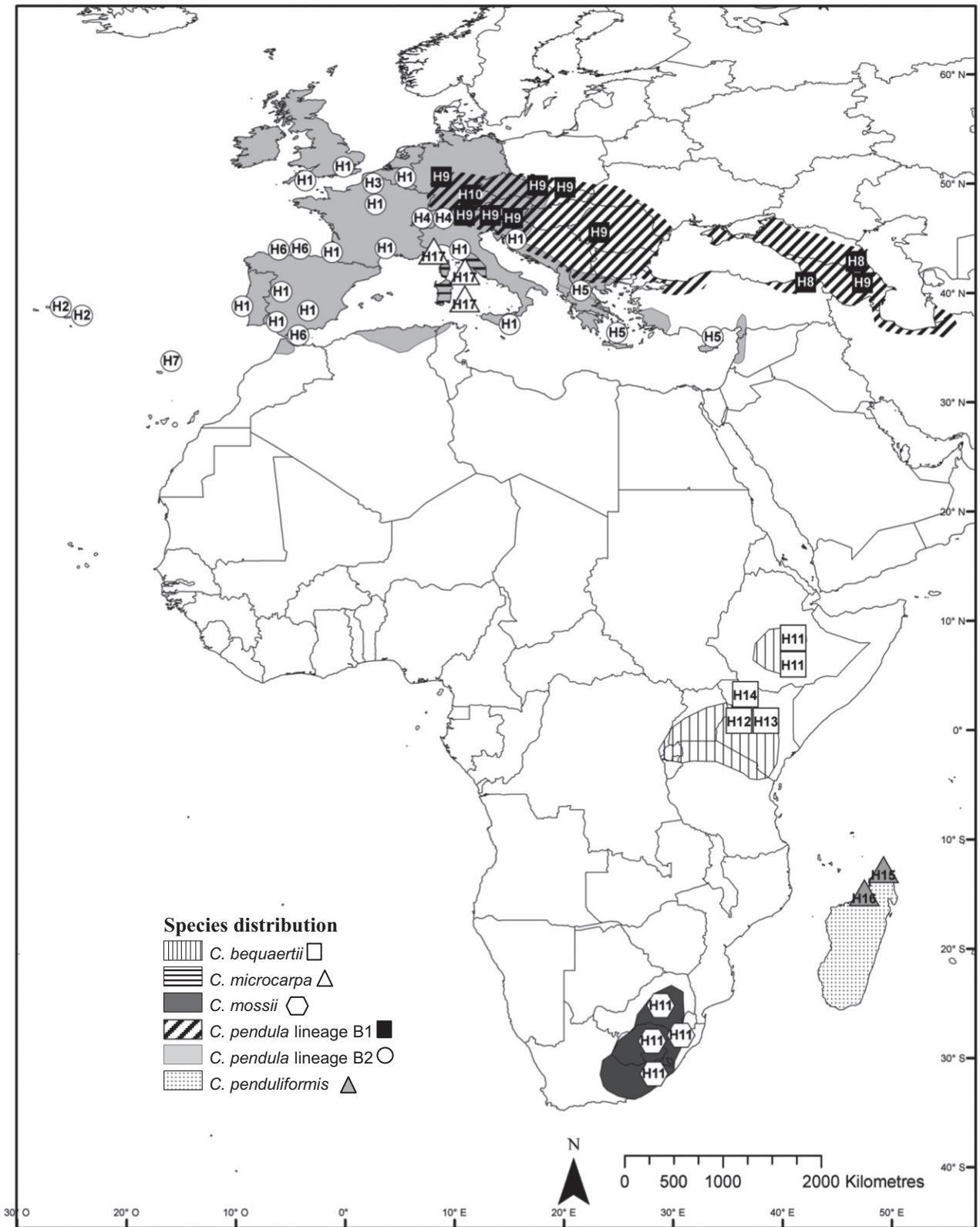


Figure 1 Distribution map of sampled populations/species and haplotypes of the species in *Carex* sect. *Rhynchosystis*. White squares are used to represent *C. bequaertii*; white triangles for *C. microcarpa*; white hexagons for *C. mossii*; black squares and white circles for *C. pendula* lineage B1 and *C. pendula* lineage B2, respectively; and grey triangles for *C. penduliformis*. The approximate distribution of the species was obtained from confirmed herbarium vouchers (Míguez *et al.*, unpublished data) and floras (Maire, 1957; Schultze-Motel, 1969; Chater, 1980; Meikle, 1985; Nilsson, 1985; Strid & Tan, 1986; Sampaio, 1988; Stace, 1997; Kukkonen, 1998; Egorova, 1999; Pignatti, 2003; Duhamel, 2004; Jermy *et al.*, 2007; Lauber & Wagner, 2007; Luceño, 2008; Jiménez-Mejías & Luceño, 2011; Zając & Zając, 2001).

fossil calibrations (Forest, 2009). Fossil records can provide only certainty for the minimum age of a clade, thus minimum age of fossil records is established as the zero offset in our analysis (see Table S3.1 in Appendix S3), as suggested by Heath (2012). Analyses were conducted using two independent Markov chain Monte Carlo (MCMC) runs of 40 million generations each, assuming a birth-death tree prior (see Appendix S3 for details). Run convergence and burn-in were assessed in TRACER 1.5 (Rambaut & Drummond, 2009). A maximum clade credibility (MCC) tree was calculated in TREEANNOTATOR 1.8.0 (Drummond *et al.*, 2012) using a posterior probability limit of 0.7 and the mean heights option (Appendix S3).

Ancestral area estimation

Biogeographical history of *Rhynchocystis* was reconstructed using dispersal–extinction–cladogenesis (DEC model utilized by Lagrange; Ree *et al.*, 2005), and likelihood implementation similar to DIVA (Ronquist, 1997) using the ‘BioGeoBEARS’ package (Matzke, 2013, 2014) in R 3.2.5 (R core team 2016), as well as Bayesian binary MCMC Analysis (BBMA) as implemented in RASP 3.2 (Yu *et al.*, 2015). In the BBMA analysis, we used 1000 randomly chosen trees from the posterior distribution of the dated tree estimated using BEAST 1.7.5 (see above), in order to assess uncertainty in biogeographical reconstructions due to both topological and temporal uncertainty (see Appendix S3). The distribution of *Rhynchocystis* was coded based on the different climatic and biogeographical regions in the Palearctic and Africa (Fig. 2, Appendix S3).

To test whether the inclusion of founder event speciation in the colonization history of the Afrotropics yielded a better model fit, a separate analysis was run only coding regions in sub-Saharan Africa and Madagascar (Appendix S3).

RESULTS

Phylogenetic analyses

A total of 82 newly generated ETS sequences, 83 ITS (73 newly generated in this study plus 10 from GenBank), 85 *matK* (83 newly generated plus 2 from GenBank) and 84 *rpl32-trnL*^{UAG} newly generated sequences were obtained (Table S1 in Appendix S1). *Rhynchocystis* constituted a well-supported clade (100% BS, 1.0 PP; Fig. 3, see also Figs S1–S4 in Appendix S2) irrespective of data matrix and analytical approach. Incongruences were found between phylogenetic reconstructions using different markers, which did not affect species relationships within *Rhynchocystis*, but the phylogenetic arrangement of different samples within species and also the relative position of outgroup (Fig. 3, and Figs S1–S4 in Appendix S2). For the sake of simplicity, we will discuss topological relationships on the basis of the topology recovered from the BI analysis of the nrDNA-ptDNA combined matrix (Fig. 3).

Rhynchocystis was arranged in two major clades (Fig. 3): Clade A (1.0 PP) included the Mediterranean *C. microcarpa* and the tropical African species *C. mossii*, *C. bequaertii* and *C. penduliformis*. *Carex microcarpa* was monophyletic (A1) and sister to the African species with strong support (100% BS, 1.0 PP). The Malagasy endemic *C. penduliformis* (A2; 1.0 PP) was recovered as sister to *C. mossii* and *C. bequaertii* (A3 and A4, respectively; Fig. 3 and Figs S1, S4, S5 and S6 in Appendix S2). The reciprocal monophyly of the latter two species lacked statistical support.

Clade B included all accessions of *C. pendula* (84% BS; 0.99 PP). This clade was formed by two subclades: B1 (78% BS; 1.0 PP) with samples of *C. pendula* from central Europe to the Caucasus and western Iran (Fig. 3); subclade B2 (95% BS; 1.0 PP) included individuals from central and western Europe, the Mediterranean basin (including northwestern Africa and Cyprus) and Macaronesia (Fig. 3). The species trees inferred using STAR (Fig. S6 in Appendix S2) showed the same supported major clades as the MP and BI trees (Fig. 3).

Phylogeographical analysis of ribotypes and haplotypes

When analysing the plastid sequences with statistical parsimony, 17 haplotypes were identified (Fig. 4). We found differences between the patterns of genealogical relationships displayed by plastid haplotypes versus nuclear ribotypes (Fig. S7 in Appendix S2). There was a higher number of ribotypes than haplotypes; the Tyrrhenian endemic *C. microcarpa* was linked to the African species in the haplotype network, whereas it appeared more closely related to *C. pendula* in the ribotype network. The species *C. bequaertii* and *C. mossii* shared H11 despite not sharing any ribotypes (Fig. 4 and Fig. S7 in Appendix S2). Haplotypes H1 to H7 belonged to lineage B2 (Figs 3 & 4) and were distributed throughout central and western Europe and the Mediterranean (Fig. 1). Haplotypes H8, H9 and H10, which corresponded to lineage B1 (Figs 3 & 4), were highly divergent with respect to lineage B2 haplotypes (at least 10 mutational connections) and were distributed throughout central Europe to the Caucasus and western Iran (Fig. 1). *Carex pendula* from Azores and Madeira and *C. microcarpa* from Corsica and Sardinia had specific haplotypes (H2 and H7, and H17, respectively; Fig. 4).

The most frequent haplotype in continental tropical Africa was H11. This haplotype was shared between *C. mossii* from South Africa and *C. bequaertii* from Ethiopia (Fig. 1). In Kenya, we found three haplotypes in *C. bequaertii* (H12, H13 and H14). *Carex penduliformis* was represented by two haplotypes (H15 and H16) with a high number of mutational connections, not only with respect to H11 but also between them.

Divergence-time estimation

Divergence of the clade comprising *Rhynchocystis* (stem node) was estimated to have occurred probably during the early Miocene (23.07 Ma, 95% highest posterior density,

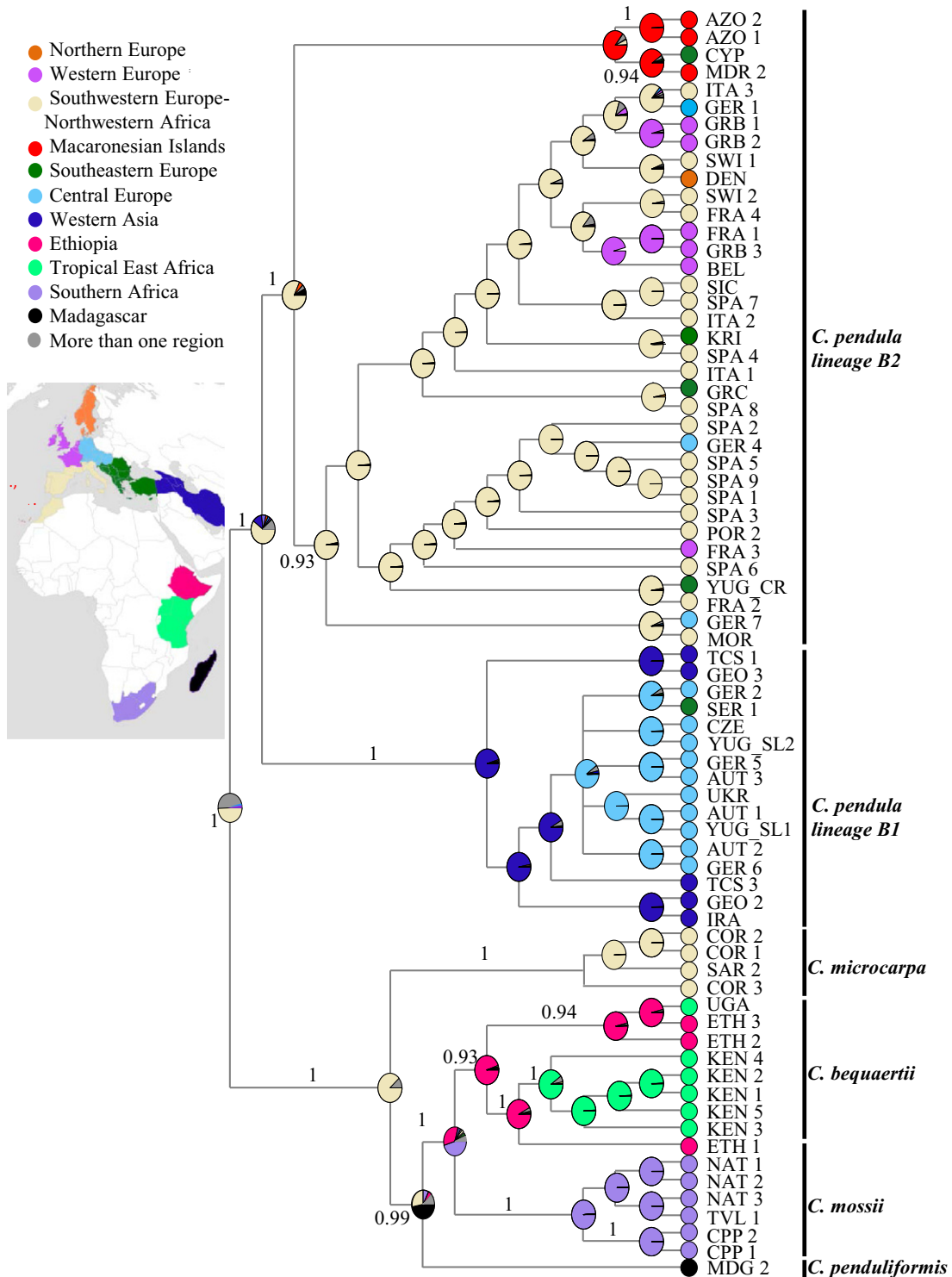


Figure 2 Ancestral area reconstructions based on the Bayesian binary Markov chain Monte Carlo (BBMA) method in RASP using the BEAST-derived chronogram of *Carex* sect. *Rhynchocystis* (see Fig. 3). Pie charts on each node indicate marginal probabilities for each alternative ancestral area derived from BBMA. Results are based on a maximum area number of eleven. Present occurrence of species is marked at the tips of the tree using the color code defined in the map top left. High posterior density (HPD at 90 %) for the divergence time estimation are shown only if posterior probability > 0.9. Outgroup taxa have been pruned. for clarity. [Colour figure can be viewed at wileyonlinelibrary.com]

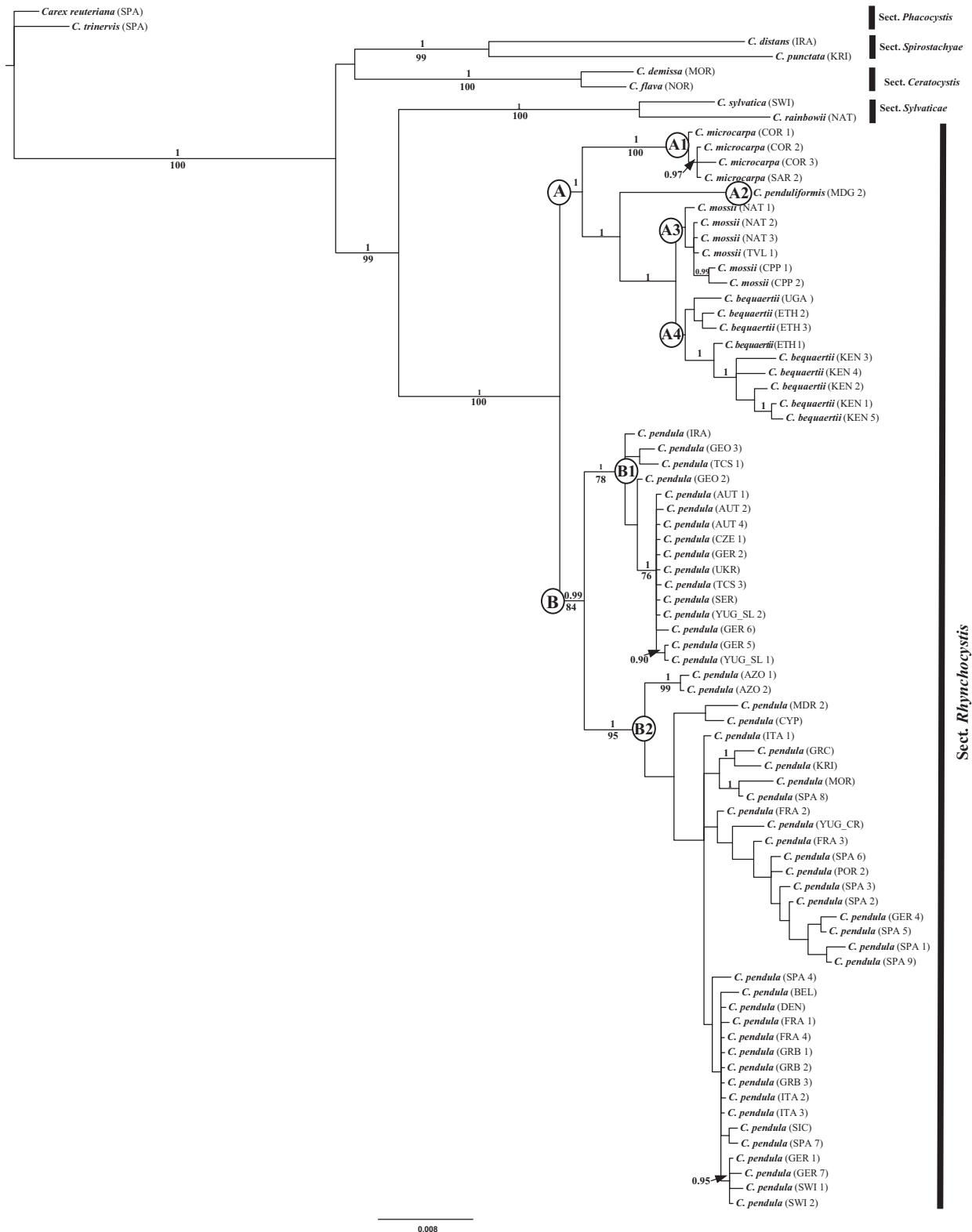


Figure 3 Majority-rule consensus tree of *Carex* sect. *Rhynchocystis* inferred under Bayesian inference using the combined nrDNA-ptDNA matrix (ETS, ITS, *matK* and *rpl32-trnL^{UAG}* regions). Numbers above and below the branches indicate clade support values: maximum parsimony bootstrap and Bayesian posterior probability, respectively. Tip labels indicate species names and codes of the source regions (in parenthesis), following ‘botanical countries’ as in Brummitt (2001), and including a number when there is more than one sample from the same region. Scale bar indicates substitutions per site.

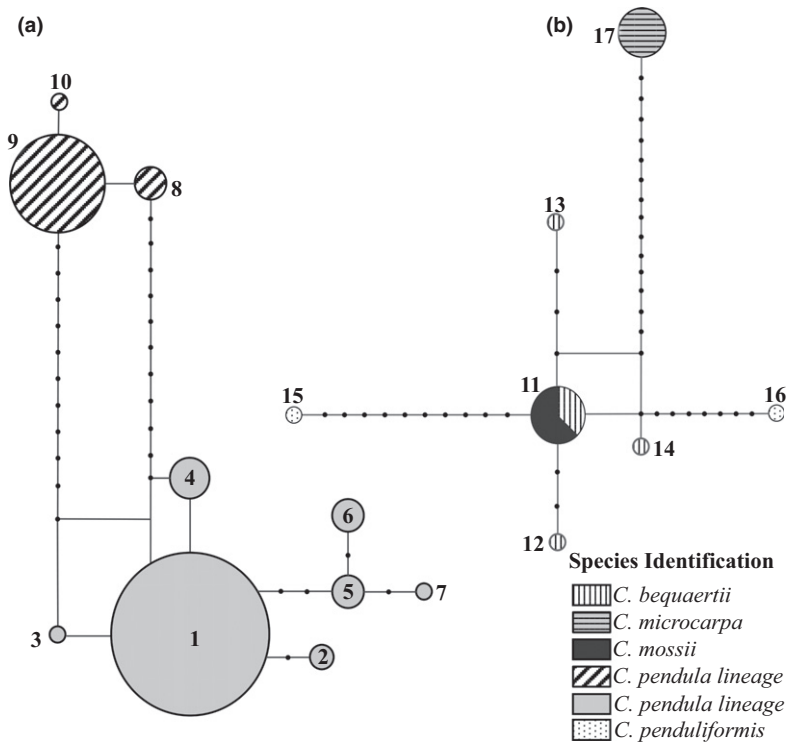


Figure 4 Statistical parsimony network of the 17 haplotypes retrieved from the analysis of the combined ptDNA matrix (*matK* and *rpl32-trnL^{UAG}*). (A) *C. pendula* network. (B) *C. microcarpa*, *C. penduliformis*, *C. mossii* and *C. bequaertii* network. Small black circles represent extinct or unsampled haplotypes, and each line between haplotypes represents a single mutational step. Circle size is proportional to the number of samples displaying the corresponding haplotype. Haplotypes for each sample are given in Appendix S1.

HPD, interval 28.6–18.36 Ma; Fig. 5, Table 2, Fig. S8 in Appendix S3). Diversification of the section (crown node) was estimated to have begun 16.32 Ma (95% HPD 17.21–15.97 Ma). Differentiation of *C. microcarpa* with respect to the African species (*C. penduliformis*, *C. bequaertii* and *C. mossii*) was estimated to have taken place around 11.54 Ma (95% HPD 15.3–7.22 Ma). Separation between the two subclades of *C. pendula* was dated to 10.14 Ma (95% HPD 15.35–4.43 Ma) (Fig. 5, Table 2; Fig. S8 in Appendix S5).

Ancestral area estimation

The biogeographical reconstruction showed similar results irrespective of the analyses performed (Appendix S3). The area of origin of the most recent common ancestor (mrca) of *Rhynchoyctis* (the crown node) and the mrca of the tropical African members of the section and *C. microcarpa* was not reconstructed with certainty although it was most likely in the southern Palaeartic (Fig. 2 and Appendix S3). Dispersal from the Palaeartic to Africa was inferred to have occurred via Madagascar or with a slightly lower likelihood twice independently, i.e. once to Madagascar (*C. penduliformis*) and once either to southern Africa (*C. mossii*) or Ethiopia (*C. bequaertii*). Tropical East Africa was probably colonized by *C. bequaertii* via Ethiopia twice independently (Fig. 2), with one colonization event seeming to have taken place in western Tropical East Africa and another in eastern Tropical East Africa.

All analyses indicated that *C. pendula* first occurred in southwestern Europe/northwestern Africa or was widespread in southern Eurasia from where it dispersed all over Europe after splitting into a western and an eastern lineage (Fig. 2).

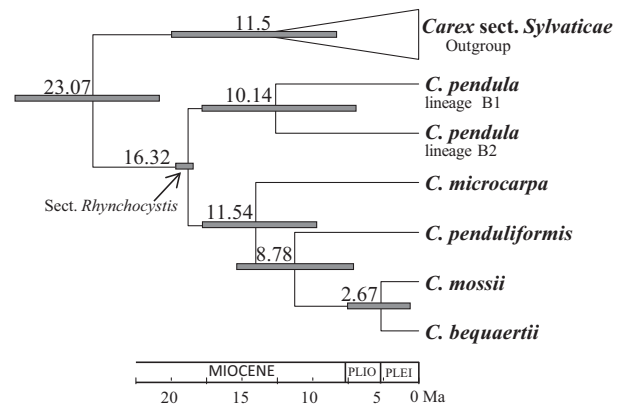


Figure 5 Summary of the maximum clade credibility tree from molecular dating analysis of *Carex* sect. *Rhynchoyctis* under an uncorrelated lognormal relaxed-clock model using a matrix of combined ETS, ITS and *matK* regions. Nodes were collapsed to summarize the main clades (see Fig. S8 in Appendix S3 for the complete tree). Mean ages are shown above the nodes. Node bars represent the 95% highest posterior density (HPD) intervals for the divergence-time estimates of each node with posterior probabilities higher than 0.9. See Table 2 for detailed ages and posterior probabilities inferred for the main clades in section *Rhynchoyctis*. PLIO, Pliocene; PLEI, Pleistocene

All scenarios in the BioGeoBEARS analyses showed the highest likelihood for DEC models with founder-effect dispersal (e.g. a daughter species occupies a range outside the distribution range of the ancestor). However, the likelihood scores of DIVA-Like models were very similar to those of the DEC+J (see Table S3.2 and Figs S9–S15 in Appendix S3).

Table 2 Divergence dates of selected clades obtained in the molecular dating analysis of *Carex* sect. *Rhynchocystis* under an uncorrelated lognormal relaxed-clock model using the combined matrix of ETS, ITS and *matK* regions in BEAST. Posterior probabilities, mean time to the most common recent ancestor in millions of years (Ma) and 95% highest posterior density (HPD) interval are shown.

Clade	Posterior probability	Mean (Ma)	95% HPD interval	
			Max.	Min.
<i>Carex</i> sect. <i>Rhynchocystis</i> (Stem node)	1	23.07	28.6	18.36
<i>Carex</i> sect. <i>Rhynchocystis</i> (Crown node)	1	16.32	17.21	15.97
Lineage A: <i>C. microcarpa</i> + <i>C. penduliformis</i> + <i>C. mossii</i> + <i>C. bequaertii</i>	1	11.54	15.3	7.22
<i>C. penduliformis</i> + <i>C. mossii</i> + <i>C. bequaertii</i>	1	8.78	12.89	4.63
<i>C. mossii</i> + <i>C. bequaertii</i>	0.99	2.67	5.03	0.62
Lineage B: <i>C. pendula</i>	0.99	10.14	15.35	4.43

DISCUSSION

Systematics of *Rhynchocystis*

Phylogenetic reconstructions of nrDNA and ptDNA regions (ETS, ITS and *matK*, *rpl32-trnL*^{UAG}, respectively) yielded partially incongruent topologies (Figs S1–S4 in Appendix S2). However, incongruences mostly affected relationships between closely related sections, as has been shown in previous studies (Waterway & Starr, 2007; Waterway *et al.*, 2009; Martín-Bravo *et al.*, 2013) and rarely within species in *Rhynchocystis*. *Rhynchocystis* species are morphologically characterized by leaf blades M-shaped in cross section, usually the widest at least 10 mm wide; culms usually longer than 90 cm; and lateral spikes 60–160(260) mm length, with more than 100 utricles per spike. *Carex pendula* and *C. microcarpa* are strongly supported as monophyletic species in the nrDNA-ptDNA combined analysis (Fig. 3), as might be expected given the undisputed taxonomy of both species (Kükenthal, 1909; Chater, 1980; Egorova, 1999). However, it is remarkable that two well-differentiated geographically distinct lineages (B1, B2; Fig. 3) were detected in *C. pendula*. Interestingly, genetic differentiation between these two *C. pendula* lineages for all studied markers is greater than between other species within lineage A (i.e. *C. mossii* versus *C. bequaertii*, *C. penduliformis* versus *C. mossii/C. bequaertii*; Fig. 4, Fig. S7 in Appendix S2). The distributions of these *C. pendula* lineages are largely allopatric (Fig. 1). Lineage B1 is distributed in C-SE Europe and SW Asia, in areas that formed the basin of the ancient Paratethys Sea (35–5 Ma). By contrast, sampled populations belonging to lineage B2 are found in the Mediterranean basin, Western Europe and Macaronesia (Azores and Madeira). Molecular phylogenetic data have allowed the detection of different taxa hidden under similar morphologies, even in apparently well-known areas

as Europe (e.g. Gurushidze *et al.*, 2008), such as in the closely related *Carex* sect. *Ceratocystis* (Jiménez-Mejías *et al.*, 2012b). Although species circumscription in *C. pendula* has not been under debate, our results could suggest the existence of unnoticed cryptic taxa within *C. pendula*. *Carex penduliformis* is a poorly known species for which only the two type populations from central Madagascar were hitherto known (Chermezon, 1937); we have studied two additional populations from northern Madagascar, which considerably expands the species range. Although Gehrke (2011) indicated the morphological similarity between *C. penduliformis*, *C. bequaertii* and *C. mossii*, there seems to be a high genetic differentiation between *C. penduliformis* and *C. bequaertii/C. mossii*, with at least nine mutational steps between their plastid haplotypes (Fig. 4). Interestingly, plastid haplotypes obtained for *C. penduliformis* populations are not only different to *C. bequaertii/C. mossii* haplotypes but also one from another (18 mutational steps; Fig. 4). *Carex mossii* and *C. bequaertii* clustered in a strongly supported monophyletic group in the nrDNA-ptDNA combined analysis (Fig. 3) and formed sister groups, the monophyly of which was, however, unsupported (see Figs S1–S4 in Appendix S2). Some populations of *C. mossii* and *C. bequaertii* shared the same, potentially ancestral, haplotype (H11; Fig. 4), which may suggest incomplete lineage sorting (Wendel & Doyle, 1998; Martín-Bravo *et al.*, 2010). Further morphological studies are needed to find clear diagnostic characters and to clarify the taxonomic status of these taxa (Míguez *et al.*, in prep.).

Persistence of *Rhynchocystis* in the Western Palaearctic since the Cenozoic

The persistence of Cenozoic relict taxa in East Asia and North America is a well-documented phenomenon, as the climatic oscillations were limited in these areas in comparison with other regions in the Northern Hemisphere (Milne & Abbott, 2002; Huang *et al.*, 2015). In Europe, many species disappeared during the Pliocene due to the progressive cooling and aridification, followed by Pleistocene glaciations, because both the mostly east–west-oriented mountain ranges and the Mediterranean Sea obstructed many species in their southwards migration to suitable habitats (Milne & Abbott, 2002). Other recent studies are providing growing evidence of Cenozoic relict lineages/species in the Western Mediterranean (e.g. *Erophaca* (Fabaceae), Casimiro-Soriguer *et al.*, 2010; *Naufraga* (Apiaceae) and *Avellara* (Asteraceae), Fernández-Mazuecos *et al.*, 2014, 2016; respectively; *Chamaerops* (Arecaceae), García-Castaño *et al.*, 2014; *Castrilanthemum* (Compositae), Tomasello *et al.*, 2015; among others).

The origin of *Rhynchocystis* dated to the early Miocene (Fig. 5) in southwestern Europe–northwestern Africa (Fig. 2, Appendix S2) is consistent with the continuous fossil record ascribed to *Rhynchocystis* in Europe through the Miocene to the Pleistocene (Jiménez-Mejías *et al.*, 2016). Therefore, the available evidence points to the persistence of *Rhynchocystis* in Europe since the late Cenozoic. The large stature, broad

leaves and preference for shady, wet habitats displayed by the extant species of the section would represent a plausible element of the Lauroid flora which may have covered the continent during this time (Barrón, 2003). Such a scenario would suggest some degree of conservation of the ecological niche in species of *Rhynchoyctis* (Wiens *et al.*, 2010).

The only previous calibrated *Carex* phylogeny that included *Rhynchoyctis* was provided by Escudero *et al.* (2012), who estimated a considerably more recent origin of the section (Late Miocene-early Pliocene), despite using a much older fossil to calibrate the stem node of *Carex* (*C. tsagajanica* Krassilov; considered highly doubtful by Jiménez-Mejías *et al.*, 2016). In our study, we also included a fossil considered to belong to *Rhynchoyctis* (Jiménez-Mejías *et al.*, 2016), although for caution we preferred to place it at the stem node of the section (see Materials and Methods). The contrasting results between these two dating approaches highlight the importance of a careful evaluation of the available fossil record for inference of reliable divergence times and therefore of explicit evolutionary/biogeographical hypotheses (Tripp & McDade, 2014).

Pre-Pleistocene phylogeographical splits in the Western Palaearctic

Speciation in the southwestern Palaearctic (e.g. Mediterranean basin and Caucasus) has frequently been attributed to Pleistocene range shifts (Médail & Diadema, 2009; Martín-Bravo *et al.*, 2010). The Mediterranean peninsulas (Iberia, Italian, Balkan, Anatolia) and islands (Balearic Islands, Corsica, Sardinia, Sicily, Crete, Cyprus) are invoked as important Pleistocene glacial refuges where species requiring warmer climates survived while the ice caps and a tundra-like environment expanded through most of Europe (Médail & Diadema, 2009; Fernández-Mazuecos *et al.*, 2014; Médail & Quezel, 2014). However, in the case of *Rhynchoyctis*, most relevant nodes are estimated to be much older (i.e. lineage A versus lineage B, *C. microcarpa* versus African lineage; *C. pendula* lineage B1 versus B2; Fig. 5). In particular, the divergence of eastern and western *C. pendula* lineages during the Middle-Upper Miocene is even older than that of *C. microcarpa* and the African species (Fig. 5).

Since the Oligocene, the Mediterranean basin has been subject to profound climatic changes, initiated with the global cooling trend (Zachos *et al.*, 2001). The closing of the Mediterranean and the Messinian salinity crisis during the late Miocene (Krijgsman *et al.*, 1999) and the establishment of a Mediterranean type climate in the early Pliocene (Suc, 1984) contributed to an aridification process (Zachos *et al.*, 2001) and the spread of steppe-like vegetation (Barrón, 2003). These events led to a dramatic change in the vegetation of southern Europe. Subtropical lauroid vegetation were replaced by Arcto-Tertiary taxa, and the most thermophilous elements largely or entirely disappeared (Ivanov *et al.*, 2011). Such changes would have promoted the retreat of species of *Rhynchoyctis* to climatically suitable areas, such as the

Tyrrhenian islands for *C. microcarpa*, SW Asia for lineage B1 of *C. pendula*, and possibly the Iberian Peninsula and/or NW Africa for lineage B2 of *C. pendula* (Fig. 1). Such results provide a picture of different parts of the Mediterranean basin acting as refugia during the Cenozoic, which contrasts with the commonly reported predominant role of the Eastern Mediterranean (Milne & Abbott, 2002). Climatic shifts during the Plio-Pleistocene may also have led to range expansions and contractions in *C. pendula*, although there is no clear evidence of ancient secondary contact between the two main lineages. Most likely, the eastern lineage (B1) underwent a severe range restriction to the eastern shores of the Paratethys (present-day southwestern Asia; Fig. 2) during the late Miocene and subsequently recolonized Europe from the East. However, the western lineage of *C. pendula* seems to have sheltered in the warmest moist climates in the Mediterranean basin (Iberian Peninsula, NW Africa), reaching also Macaronesia (apparently by at least two independent dispersals to the Azores and Madeira archipelagos; Fig. 2). It migrated from its refuge areas to central, northern and western Europe during the range expansion–contraction cycles associated with Plio-Pleistocene climatic fluctuations.

A Rand Flora pattern in *Rhynchoyctis* originated via long-distance dispersal facilitated by Mio-Pliocene global cooling

Our results suggest a scenario of long-distance dispersal from the Mediterranean to sub-Saharan Africa (Fig. 2 and Appendix S3) as the most likely explanation for the colonization of the Afrotropics. Long-distance dispersal events have been proposed to explain disjunct distributions between the Palaearctic and sub-Saharan Africa in *Carex* (Gehrke & Linder, 2009; Martín-Bravo & Escudero, 2012; Gizaw *et al.*, 2016), *Geranium* L. (Geraniaceae; Fiz *et al.*, 2008), *Lychnis* L. (Caryophyllaceae; Popp *et al.*, 2008) and other plant species (Gehrke & Linder, 2014; Linder, 2014). The inferred colonization of the Afrotropics from the Palaearctic seems to have taken place during the late Miocene (Table 2, Fig. 5). It coincides with three major events that affected the area: (1) worldwide cooling (Schuster *et al.*, 2006); (2) increasing aridity in northern Africa, which led to the origin of the Sahara Desert (11.6–7.2 Ma; Zhang *et al.*, 2014); and (3) the uplift of the Eastern Arc Mountains (8–7 Ma; Sepulchre *et al.*, 2006). It should be noted that our results do not rule out colonization of east Africa from the Palaearctic with the Arabian mountains as stepping-stones and subsequent extinction in this part of SW Asia. This alternative vicariance hypothesis has been demonstrated in other plant groups (Assefa *et al.*, 2007; Popp *et al.*, 2008; Thiv *et al.*, 2010; Mairal *et al.*, 2015; Pokorný *et al.*, 2015). However, under this scenario, we would have expected a closer relationship of the African plants to lineage B1 of *C. pendula*, as this lineage was presumably present in SW Asia during the period the colonization occurred. In addition, none of our inferred biogeographical scenarios invokes the past presence of the African lineage in SW Asia.

Interestingly, colonization of the Afrotropical regions via Madagascar as suggested as one possible scenario in our analyses has not been reported in the literature before (Fig. 2). In addition, the haplotype network (Fig. 4B) suggests the presence of the ancestral haplotype (H11; Fig. 4) in two disjunct areas of mainland Africa (Fig. 1): the Simien Mountains (Ethiopia) and the Drakensberg (eastern South Africa). Moreover, two haplotypes which occur in Madagascar appear to be derived from those on the mainland (Fig. 4). This points to an initial colonization of eastern Africa and subsequently dispersal to Madagascar (at least twice), instead of the other way round as represented in the most likely ancestral area reconstruction (Fig. 2).

ACKNOWLEDGEMENTS

This work was funded by the Spanish Ministry of Economy and Competitiveness through the project CGL2016-77401 and the National Science Foundation (award no. 1256033). The authors thank M. Sequeira, M. Spencer, H. Schaefer, A. Reznicek and M. Urbani for providing plant material and Michael Pirie for reviewing the English. We also thank the curators and staff from herbaria B, E, M, MHA, MADJ, UPOS, UPS, US, P, PRE, SEV, SS, TUM and Z, for granting us access to their collections and for providing plant material; and to F.J. Fernández (UPOS) for technical support.

REFERENCES

- Alarcón, M., Roquet, C., García-Fernández, A., Vargas, P. & Aldasoro, J. J. (2013) Phylogenetic and phylogeographic evidence for a Pleistocene disjunction between *Campanula jacobaea* (Cape Verde Islands) and *C. balfourii* (Socotra). *Molecular Phylogenetics and Evolution*, **69**, 828–836.
- Assefa, A., Ehrlich, D., Taberlet, P., Nemomissa, S. & Brochmann, C. (2007) Pleistocene colonization of afro-alpine 'sky islands' by the arctic-alpine *Arabis alpina*. *Heredity (Edinb)*, **99**, 133–142.
- Barrón, E. (2003) Evolución de la Flora Terciaria en la Península Ibérica. *Monografías del jardín botánico de Córdoba*, **74**, 63–74.
- Brummitt, R. K. (2001) *World Geographical Scheme for Recording Plant Distributions Edition 2*. Hunt Institute for Botanical Documentation, Carnegie Mellon University, Pittsburgh, Pennsylvania, USA.
- Casimiro-Soriguer, R., Talavera, M., Balao, F., Terrab, A., Herrera, J. & Talavera, S. (2010) Phylogeny and genetic structure of *Erophaca* (Leguminosae), a East-West Mediterranean disjunct genus from the Tertiary. *Molecular Phylogenetics and Evolution*, **56**, 441–450.
- Chandler, M. E. J. (1963) Revision of the Oligocene floras of the Isle of Wight. *Bulletin of the British Museum (Natural History)*. *Geology*, **6**, 321–384.
- Chater, A. O. (1980) *Carex. Flora Europaea* (ed. by T. G. Tutin, V. H. Heywood, N. A. Burges, D. M. Moore, S. M. Walters and D. A. Webb), pp. 290–302. Cambridge University Press, Cambridge.
- Chen, C., Qi, Z. C., Xu, X. H., Comes, H. P., Koch, M. A., Jin, X. J., Fu, C. X. & Qiu, Y. X. (2014) Understanding the formation of Mediterranean-African-Asian disjunctions: evidence for Miocene climate-driven vicariance and recent long-distance dispersal in the Tertiary relict *Smilax aspera* (Smilacaceae). *New Phytologist*, **204**, 243–255.
- Chermezon, H. (1937) *Cyperaceae: Schoenoxiphium; Carex. Flore de Madagascar (Plantes Vasculaires)* (ed. by H. Humbert), pp. 272–299.
- Christ, H. (1910) *Die Geographie der Farne*. Verlag von Gustav Fischer, Jena.
- Clement, M., Posada, D. & Crandall, K. A. (2000) TCS: a computer program to estimate gene genealogies. *Molecular Ecology*, **9**, 1657–1659.
- Dai, L. K., Koyama, T. (2010) *Carex* sect. *Graciles* Kük (ed. by I. A. Al-Shehbaz *et al.*), Missouri Botanical Garden Press, St. Louis, Missouri, USA.
- Drummond, A. J., Suchard, M. A., Xie, D. & Rambaut, A. (2012) Bayesian phylogenetics with BEAUti and the BEAST 1.7. *Molecular Biology and Evolution*, **29**, 1969–1973.
- Duhamel, G. (2004) *Flore et Cartographie des Carex de France*. Paris.
- Egorova, T. (1999) *The sedges (Carex L.) of Russia and adjacent states (within the limits of the former USSR)*. Missouri Botanical Garden Press, St. Louis, Missouri, USA.
- Escudero, M., Valcárcel, V., Vargas, P. & Luceño, M. (2009) Significance of ecological vicariance and long-distance dispersal in the diversification of *Carex* sect. *Spirostachyae* (Cyperaceae). *American Journal of Botany*, **96**, 2100–14.
- Escudero, M., Hipp, A. L., Waterway, M. J. & Valente, L. M. (2012) Diversification rates and chromosome evolution in the most diverse angiosperm genus of the temperate zone (*Carex*, Cyperaceae). *Molecular Phylogenetics and Evolution*, **63**, 650–5.
- Fernández-Mazuecos, M., Jiménez-Mejías, P., Rotllan-puig, X. & Vargas, P. (2014) Narrow endemics to Mediterranean islands: moderate genetic diversity but narrow climatic niche of the ancient, critically endangered *Naufraga* (Apiaceae). *Journal of PPEES Sources*, **16**, 190–202.
- Fernández-Mazuecos, F., Jiménez-Mejías, P., Martín-Bravo, S., Buide, M. L., Álvarez, I. & Vargas, P. (2016) Narrow endemics on coastal plains: Miocene divergence of the critically endangered genus *Avellara* (Compositae). *Plant Biology*, **18**, 729–738.
- Fiz, O., Vargas, P., Alarcón, M., Aedo, C., García, J. L. & Aldasoro, J. J. (2008) Phylogeny and historical biogeography of Geraniaceae in relation to climate changes and pollination ecology. *Systematic Botany*, **33**, 326–342, 789–794.
- Forest, F. (2009) Calibrating the tree of life: fossils, molecules and evolutionary timescales. *Annals of Botany*, **104**, 789–794.
- García-Castaño, J. L., Terrab, A., Ortiz, M. Á., Stuessy, T. F. & Talavera, S. (2014) Patterns of phylogeography and vicariance of *Chamaerops humilis* L. (Palmae). *Turkish Journal of Botany*, **38**, 1132–1146.

- Gehrke, B. (2011) Synopsis of *Carex* (Cyperaceae) from sub-Saharan Africa and Madagascar. *Botanical Journal of the Linnean Society*, **166**, 51–99.
- Gehrke, B. & Linder, H. P. (2009) The scramble for Africa: pan-temperate elements on the African high mountains. *Proceedings Biological Sciences/The Royal Society*, **276**, 2657–65.
- Gehrke, B. & Linder, H. P. (2014) Species richness, endemism and species composition in the tropical Afroalpine flora. *Alpine Botany*, **124**, 165–177.
- Gehrke, B., Martín-Bravo, S., Muasya, M. & Luceño, M. (2010) Monophyly, phylogenetic position and the role of hybridization in *Schoenoxiphium* Nees (Cariceae, Cyperaceae). *Molecular Phylogenetics and Evolution*, **56**, 380–92.
- Gizaw, A., Wondimu, T., Mugizi, T. F., Masao, C. A., Abdi, A. A., Popp, M., Ehrlich, D. & Nemomissa, S. (2016) Vicariance, dispersal, and hybridization in a naturally fragmented system: the afro-alpine endemics *Carex monostachya* and *C. runsoroensis* (Cyperaceae). *Alpine Botany*, 1–13.
- Global Carex Group (2016) Megaphylogenetic specimen-level approaches to the *Carex* (Cyperaceae) phylogeny using ITS, ETS, and *matK* sequences: systematics implications. *Systematic Botany*, **41**, 500–518.
- Gurushidze, M., Fritsch, R. M. & Blattner, F. R. (2008) Phylogenetic analysis of *Allium* subg. *Melanocrommyum* infers cryptic species and demands a new sectional classification. *Molecular Phylogenetics and Evolution*, **49**, 997–1007.
- Heath, T. A. (2012) A hierarchical bayesian model for calibrating estimates of species divergence times. *Systematic Biology*, **61**, 793–809.
- Huang, Y., Jacques, F. M. B., Su, T., Ferguson, D. K., Tang, H., Chen, W. & Zhou, Z. (2015) Distribution of Cenozoic plant relicts in China explained by drought in dry season. *Nature Publishing Group*, 1–7.
- Ivanov, D., Utescher, T., Mosbrugger, V., Syabryaj, S., Djordjević-Milutinović, D. & Molchanoff, S. (2011) Miocene vegetation and climate dynamics in Eastern and Central Paratethys (Southeastern Europe). *Palaeogeography, Palaeoclimatology, Palaeoecology*, **304**, 262–275.
- Jermey, A., Simpson, D., Foley, M. J. & Porter, M. (2007) *Sedges of The British Island*. Botanical Society of the British Isles, London.
- Jiménez-Mejías, P. & Luceño, M. (2011) Cyperaceae. In: Euro+Med Plantbase. <http://ww2.bgbm.org/EuroPlusMed/> [2014].
- Jiménez-Mejías, P., Escudero, M., Guerra-Cárdenas, S., Lye, K. A. & Luceño, M. (2011) Taxonomic delimitation and drivers of speciation in the Ibero-North African *Carex* sect. *Phacocystis* river-shore group (Cyperaceae). *American Journal of Botany*, **98**, 1855–67.
- Jiménez-Mejías, P., Luceño, M., Lye, K. A., Brochmann, C. & Gussarova, G. (2012a) Genetically diverse but with surprisingly little geographical structure: the complex history of the widespread herb *Carex nigra* (Cyperaceae). *Journal of Biogeography*, **39**, 2279–2291.
- Jiménez-Mejías, P., Martín-Bravo, S. & Luceño, M. (2012b) Systematics and taxonomy of *Carex* sect. *Ceratocystis* (Cyperaceae) in Europe: a molecular and cytogenetic approach. *Systematic Botany*, **37**, 382–398.
- Jiménez-Mejías, P., Martinetto, E., Momohara, A., Popova, S., Smith, S. Y. & Roalson, E. H. (2016) A commented synopsis of the pre-Pleistocene fossil record of *Carex* (Cyperaceae). *The Botanical Review*, **82**, 258–345.
- Kondraskov, P., Schütz, N., Schüßler, C., de Sequeira, M. M., Guerra, A. S., Caujapé-Castells, J., Jaén-Molina, R., Marrero-Rodríguez, Á., Koch, M. A., Linder, P., Kovar-Eder, J. & Thiv, M. (2015) Biogeography of Mediterranean hotspot biodiversity: re-evaluating the “Tertiary Relict” hypothesis of Macaronesian laurel forests. *PLoS ONE*, **10**, e0132091.
- Krijgsman, W., Hilgen, F. J., Raffi, I., Sierro, F. J. & Wilson, D. S. (1999) Chronology, causes and progression of the Messinian salinity crisis. *Nature*, **400**, 652–655.
- Kroepelin, S. (2006) Revisiting the age of the Sahara Desert. *Science*, **312**, 1138–1139.
- Kükenthal, G. (1909) *Cyperaceae-Caricoidae*. Das Pflanzenreich, IV, 20 (Heft 38). W. Englemann, Leipzig.
- Kukkonen, I. (1998) Cyperaceae. *Flora Iranica* (ed. by K. Rechinger), pp. 307. Akademische Druck u. Verlagsanstalt, Graz.
- Lauber, K. & Wagner, G. (2007) *Flora Helvetica*. Berlin, Germany.
- Linder, H. P. (2014) The evolution of African plant diversity. *Frontiers in Ecology and Evolution*, **2**, 1–14.
- Liu, L., Yu, L., Pearl, D. K. & Edwards, S. V. (2009) Estimating species phylogenies using coalescence times among sequences. *Systematic Biology*, **58**, 468–477.
- Luceño, M. (2008) *Carex* sections *Rhynchocystis* and *Sylvaticae* Rouy. *Flora Iberica*. Vol. 18 (ed. by S. Castroviejo et al.), pp. 163–167. CSIC, Madrid.
- Maguilla, E., Hipp, A. L., Waterway, M. J., Hipp, A. L. & Luceño, M. (2015) Phylogeny, systematics, and trait evolution of *Carex* section *Glareosae*. *American Journal of Botany*, **102**, 1128–1144.
- Mairal, M. & Sánchez-Meseguer, A. (2012) Resolviendo una incógnita biogeográfica, el caso de la Rand Flora afro-mediterránea. *Chronica Naturae*, **2**, 53–63.
- Mairal, M., Pokorný, L., Aldasoro, J. J., Alarcón, M. & Sanmartín, I. (2015) Ancient vicariance and climate-driven extinction explain continental-wide disjunctions in Africa: the case of the Rand Flora genus *Canarina* (Campanulaceae). *Molecular Ecology*, **24**, 1335–54.
- Maire, R. (1957) *Flore de l'Afrique du Nord IV* (ed. by Lechevalier). Paris.
- Martín-Bravo, S. & Escudero, M. (2012) Biogeography of flowering plants: a case study in mignonettes (Resedaceae) and sedges (*Carex*, Cyperaceae) (ed. by L. Stevens), pp. 257–290. Intech, Rijeka, Croatia.
- Martín-Bravo, S., Valcárcel, V., Vargas, P. & Luceño, M. (2010) Geographical speciation related to Pleistocene range shifts in the western Mediterranean mountains (*Reseda* sect. *Glaucoreseda*, Resedaceae). **59**, 466–482.
- Martín-Bravo, S., Escudero, M., Míguez, M., Jiménez-Mejías, P. & Luceño, M. (2013) Molecular and morphological

- evidence for a new species from South Africa: *Carex rainbowii* (Cyperaceae). *South African Journal of Botany*, **87**, 85–91.
- Matzke, N. J. (2013) BioGeoBEARS: BioGeography with Bayesian (and Likelihood). Evolutionary Analysis in R Scripts. Release R package version 0.2.1. <http://CRAN.R-project.org/package=BioGeoBEARS>.
- Matzke, N. J. (2014) Model selection in historical biogeography reveals that founder event speciation is a crucial process in island clades. *Systematic Biology*, **63**, 951–970.
- Médail, F. & Diadema, K. (2009) Glacial refugia influence plant diversity patterns in the Mediterranean Basin. *Journal of Biogeography*, **36**, 1333–1345.
- Médail, F. & Quezel, P. (2014) Hot-spots analysis for conservation of plant biodiversity in the Mediterranean basin. *Annals of the Missouri Botanical Garden*, **84**, 112–127.
- Meikle, R. D. (1985) *Flora of Cyprus* Vol. II (ed. by R. D. Meikle). Royal Botanical Gardens, London.
- Milne, R. I. & Abbott, R. J. (2002) The origin and evolution of tertiary relict floras. *Advances in Botanical Research*, **38**, 281–314.
- Nelmes, E. (1940) Notes on *Carex* XIII. – African allies of *C. pendula* Huds. *Kew Bulletin*, **1940**, 135–137.
- Nilsson, Ö. (1985) *Carex* L. *Flora of Turkey*. 9 (ed. by P. Davis), pp. 73–158. Edinburgh University Press, Edinburgh.
- Parham, J. F., Donoghue, P. C. J., Bell, C. J. *et al.* (2012) Best practices for justifying fossil calibrations. *Systematic Biology*, **61**, 346–359.
- Pignatti, S. (2003) *Flora d'Italia*. Vol. 3. Edagricole, Bologna.
- Pokorný, L., Riina, R., Mairal, M., Meseguer, A. S., Culshaw, V., Cendoya, J., Serrano, M., Carbajal, R., Ortiz, S., Heuertz, M. & Sanmartín, I. (2015) Living on the edge: timing of Rand Flora disjunctions congruent with ongoing aridification in Africa. *Frontiers in Genetics*, **6**, 1–15.
- Popp, M., Gizaw, A., Nemomissa, S., Suda, J. & Brochmann, C. (2008) Colonization and diversification in the African “sky islands” by Eurasian *Lychnis* L. (Caryophyllaceae). *Journal of Biogeography*, **35**, 1016–1029.
- Rambaut, A. & Drummond, A. J. (2009) Tracer version 1.5. Available at: <http://beast.bio.ed.ac.uk>.
- Ree, R. H., Moore, B. R., Webb, C. O. & Donoghue, M. J. (2005) A likelihood framework for inferring the evolution of geographic range on phylogenetic trees. *Evolution*, **59**, 2299–2311.
- Reznicek, A. A. (2001) Sectional names in *Carex* (Cyperaceae) for the flora of North America. *Novon*, **11**, 454–459.
- Ronquist, F. (1997) Dispersal-vicariance analysis: a new approach to the quantification of historical biogeography. *Systematic Biology*, **46**, 195–203.
- Sampaio, G. (1988) *Flora Portuguesa*. Lisboa.
- Sanmartín, I., Anderson, C. L., Alarcon, M., Ronquist, F. & Aldasoro, J. J. (2010) Bayesian island biogeography in a continental setting: the Rand Flora case. *Biology Letters*, **6** (5), 703–707.
- Schultze-Motel, W. (1969) *Carex* L. In: HEGI, A. *Illustrierte Flora von Mitteleuropa* ed. 3, 1/II: 96–274. Dritte, völlig neubearbeitete Auflage. Verlag P. Parey, Berlin, Hamburg.
- Schuster, M., Durringer, P., Ghienne, J.-F., Vignaud, P., Mackaye, H. T., Likius, A. & Brunet, M. (2006) The age of the Sahara Desert. *Science*, **311**, 821.
- Sepulchre, P., Ramstein, G., Fluteau, F., Schuster, M., Tiercelin, J.-J. & Brunet, M. (2006) *Science*, **313**, 1419–1423.
- Shaw, J., Lickey, E. B., Schilling, E. E. & Small, R. L. (2007) Comparison of whole chloroplast genome sequences to choose noncoding regions for phylogenetic studies in angiosperms: the tortoise and the hare III. *American Journal of Botany*, **94**, 275–288.
- Shaw, T. I., Ruan, Z., Glenn, T. C. & Liu, L. (2013) STRAW: Species Tree Analysis Web server. *Nucleic Acids Research*, **41**, 238–241.
- Stace, C. (1997) *New flora of the British Isles*. Cambridge University Press, Bath.
- Starr, J. R., Naczi, R. F. C. & Chouinard, B. N. (2009) Plant DNA barcodes and species resolution in sedges (*Carex*, Cyperaceae). *Molecular Ecology Resources*, **9** (Suppl s1), 151–163.
- Strid, A. & Tan, K. (1986) *Mountain Flora of Greece*. Vol. 2. Edinburgh University Press, Edinburgh.
- Suc, J. P. (1984) Origin and evolution of the Mediterranean vegetation and climate in Europe. *Nature*, **307**, 429–432.
- Thiers, B. (2015) Index Herbariorum: a global directory of public herbaria and associated staff. New York Botanical Garden's Virtual Herbarium. <http://sweetgum.nybg.org/ih/> (continuously updated).
- Thiv, M., Thulin, M., Hjertson, M., Kropf, M. & Linder, H. P. (2010) Evidence for a vicariant origin of Macaronesian-Eritrean/Arabian disjunctions in *Campylanthus* Roth (Plantaginaceae). *Molecular Phylogenetics and Evolution*, **54**, 607–616.
- Tomasello, S., Álvarez, I., Vargas, P. & Oberprieler, C. (2015) Is the extremely rare Iberian endemic plant species *Castri-lanthemum debeauxii* (Compositae, Anthemideae) a “living fossil”? Evidence from a multi-locus species tree reconstruction. *Molecular Phylogenetics and Evolution*, **82**, 118–130.
- Tripp, E. A. & McDade, L. A. (2014) A rich fossil record yields calibrated phylogeny for Acanthaceae (Lamiales) and evidence for marked biases in timing and directionality of intercontinental disjunctions. *Systematic Biology*, 1–25.
- Valtuena, F. J., Preston, C. D. & Kadereit, J. W. (2012) Phylogeography of a Tertiary relict plant, *Meconopsis cambrica* (Papaveraceae), implies the existence of northern refugia for a temperate herb. *Molecular Ecology*, **21**, 1423–37.
- Waterway, M. J. & Starr, J. R. (2007) Phylogenetic relationships in tribe *Cariceae* (Cyperaceae) based on nested analyses of four molecular data sets. *Aliso*, **23**, 165–192.
- Waterway, M. J., Hoshino, T. & Masaki, T. (2009) Phylogeny, species richness, and ecological specialization in Cyperaceae tribe *Cariceae*. *The Botanical Review*, **75**, 138–159.
- Weijermars, R. (1988) Neogene tectonics in the Western Mediterranean may have caused the Messinian salinity

- crisis and an associated glacial event. *Tectonophysics*, **148**, 211–219.
- Wendel, J. F. & Doyle, J. J. (1998) Phylogenetic incongruence: window into genome history and molecular evolution. *Molecular Systematics of Plants II* (ed. by D.E. Soltis, P.S. Soltis and J.J. Doyle), pp. 265–296. Springer, US.
- Wiens, J. J., Ackerly, D. D., Allen, A. P., Anacker, B. L., Buckley, L. B., Cornell, H. V., Damschen, E. I., Jonathan, Davies T., Grytnes, J.-A., Harrison, S. P., Hawkins, B. A., Holt, R. D., McCain, C. M. & Stephens, P. R. (2010) Niche conservatism as an emerging principle in ecology and conservation biology. *Ecology Letters*, **13**, 1310–1324.
- Yu, Y., Harris, A. J., Blair, C. & He, X. (2015) RASP (Reconstruct Ancestral State in Phylogenies): a tool for historical biogeography. *Molecular Phylogenetics and Evolution*, **87**, 46–49.
- Zachos, J., Pagani, M., Sloan, L., Thomas, E. & Billups, K. (2001) Trends, rhythms, and aberrations in global climate 65 Ma to present.
- Zajac, M. & Zajac, A. (2001) *Distribution atlas of vascular plants in Poland* (ed by M. Zajac and A. Zajac). Laboratory of Computer Chorology, Institute of Botany, Jagiellonian University, Kraków.
- Zhang, Z., Ramstein, G., Schuster, M., Li, C., Contoux, C. & Yan, Q. (2014) Aridification of the Sahara Desert caused by Tethys Sea shrinkage during the Late Miocene. *Nature*, **513**, 401–4.

SUPPORTING INFORMATION

Additional Supporting Information may be found in the online version of this article:

Appendix S1. List of studied material.

Appendix S2. Supplementary figures.

Appendix S3. Additional methodological details.

BIOSKETCH

Mónica Míguez is a Ph.D student at Pablo de Olavide University, Seville (Spain). Her research is focused on the evolution of angiosperms, with special interest in the systematics and biogeography of the genus *Carex* (Cyperaceae).

Author contributions: P.J.-M. and S.M.-B. conceived the idea, collected plant material and drafted the manuscript; E.M. and B.G. analysed data and collected plant material; M.M. carried out the laboratory work, analysed the data and led the writing. All authors contributed to the writing of the final version.

Editor: Liliana Katinas